SAND2012-1895C

The Science, Technology, and Applications of Terawatt-Class Pulsed Power Drivers at Sandia National Laboratories

M. K. Matzen, M. G. Mazarakis, J. E. Bailey, M. E. Cuneo, M. P. Desjarlais, S. F. Glover, M. C. Herrmann, B. M. Jones, M. D. Knudson, J. J. Leckbee, , B. V. Oliver, J. L. Porter, G. A. Rochau, L. X. Schneider, D. B. Sinars W. A. Stygar, M. A. Sweeney, R. A. Vesey, and J. R. Woodworth.

Sandia National Laboratories Albuquerque, N.M. 87185 USA

Abstract— There has been significant progress in the past few years in the development and application of Terawatt-class pulsed power generators. Sandia's flagship is the Z facility, which was recently refurbished to improve its energy, power (~100 TWe), reliability, and precision. We are now routinely performing one shot per day, obtaining load currents as high as 26 MA to create high magnetic fields (> 1000 Tesla) and pressures (10s of Mbar). In a z-pinch configuration, the magnetic pressure (Lorentz Force) supersonically implodes a plasma created from a cylindrical wire array or liner, which at stagnation generates a plasma with energy densities as high as 10 MJ/cm^3 and temperatures exceeding 1 keV at 0.1% of solid density. These plasma implosions can produce over 2 MJ of x-ray energy at powers greater than 200 TW for Inertial Confinement Fusion (ICF), radiation hydrodynamics, radiation-material interaction, Inertial Fusion Energy (IFE), and astrophysics experiments. In an alternate configuration, the large magnetic pressure is used to directly drive Isentropic Compression Experiments (ICE) to pressures greater than 6 Mbar or accelerate flyer plates to velocities as high as 45 km/s for equation of state experiments at pressures as high as 20 Mbar. This research and development is performed in collaboration with many other research groups from large laboratories and universities around the world. This paper summarizes research performed with Z and more recently with the refurbished Z facility, advances in high-photon-energy radiography, derivative applications of the pulsed power program, and advances in the science of pulsed power that could revolutionize the next-generation facilities.

I. INTRODUCTION

Pulsed power science is a collection of technologies, capabilities, and theoretical and experimental tools that enable us to concentrate, in an efficient manner, large amounts of electrical energy in space and time. Our objective is to create and understand high energy density environments (Mbar pressures, keV x-ray radiation energies, etc.) by conducting highly diagnosed experiments in the following areas: magnetically-driven plasma implosions; magnetically-driven compression waves and flyer plate acceleration; intense and high average-power particle beam generation, transport and focusing; high-voltage breakdown phenomenology; and electrostatic discharge physics. The capabilities that enable these applications are large-scale computations, theory, advanced diagnostics, and the ability to do precision measurements. The large scale pulsed power facilities at Sandia National Laboratories available for experiments are the Z pulsed power facility (26 MA, 100 TW, 100 to 300 ns), the Z-Beamlet (2 TW, 1 ns) and Z-Petawatt (4 PW, ps) laser facilities (Fig. 1), the Radiographic Integrated Test Stand (RITS) facility (120-180 kA, 10 MeV, 55 ns), the radiographic Linear Transformer Driver (LTD) accelerator (1-3 MeV, 100 kA, 50 ns), and the Mykonos LTD accelerator (1-2 TW, 1 MA, 90 ns).

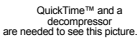

Fig. 1 Top view of the Z, Petawatt and Beamlet compound.

The Z generator in particular is the largest multi-terawatt high current driver capable of generating extreme high energy density physics conditions and thus enabling the laboratory study of magnetically driven plasma implosions, magnetically driven compression waves and flyer plate acceleration.

With such a suite of capabilities and facilities we have been able to address many High Energy Density Science (HEDS) applications such as inertial confinement fusion (ICF), Inertial Fusion Energy (IFE),

the physics of materials under high pressure, and astrophysics. Spin-off applications include three-dimensional (3D) electromagnetic simulations of large systems that require massively parallel computer resources, engineering of inertial fusion energy systems, and high-brightness flash x-ray radiography. We are also developing new pulsed power techniques that will enable major advances in future accelerator architecture.

II. THE Z FACILITY

The Z accelerator, from the very first shot, has proven to be a very successful experimental platform for HEDS, ICF, radiation hydrodynamics, radiation-material interaction, IFE, and astrophysics.

In the last few years, the refurbished Z accelerator augmented those capabilities and provided more accurate diagnostics and a higher concentration of energy and power into various loads. The first shot on Z was in September 1996. The last shot before shutdown for the refurbishment project was in July, 2006. Z had operated at up to 20 MA and 50 TW on over 1700 shots. The results from these experiments have been published in over 160 peer reviewed journal articles. A detailed description of Z architecture can be found in numerous publications [1-9].

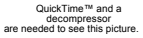

Fig. 2. The refurbished Z driver. The improvements in various machine sections are indicated.

The refurbished Z kept the same basic architecture while incorporating a number of very important major improvements and enhancements depicted in Fig. 2 including:

- new Marx generator capacitors, doubling the energy storage capability within the same capacitor volume;
- individual lasers for the triggered gas switches, providing the main pulse shaping capability;
- intermediate storage capacitors electrically optimized for a balance between short pulse mode (100 ns) and long pulse mode for material property experiments, with high electrical reliability in either mode;
- a laser triggered gas switch located in oil to reduce the likelihood of electrical breakdown;
- a single stage electrically optimized pulse forming line, replacing the three stage hardware from the original Z system;
- an updated power flow section incorporating several features that will reduce maintenance and enhance reliability;
- steeper angled magnetically insulated transmission lines providing a horizontal line of sight capability, debris mitigation features, new current gaskets, and expanded current diagnostic capability; and
- stainless steel components for durability and reduced maintenance leading to reduced shot turn around.

The upgraded pulsed power system of the refurbished Z [10-12] is capable now of delivering more than nine mega-joules of forward going wave energy in the first one hundred nanoseconds of its pulse. As it was in the original Z, the system is composed of thirty-six nominally identical modules, each producing a 3.3-terawatt pulse in 6 Ω water-insulated transmission lines. The peak forward-going voltage is of the order of 5 MV. The nominal pulse rise time is ~75 ns, and the full width at half maximum is ~190 ns. However, the pulse shape and FWHM can also be changed between 100 and 600 ns in order to accommodate a large variety of ICF, Isentropic Compression Experiments (ICE) and astrophysics experiments. The thirty-six modules are combined in parallel and drive up to 26 MA into a single load.

The refurbished Z was put into service on September 27, 2007. Following a brief commissioning period the generator now operates flawlessly averaging one shot per day at up to 26 MA maximum current depending on load inductance. More than 360 shots have been fired up to now demonstrating a substantial accelerator enhancement in precision, capacity, and capability. One of the key factors of these achievements was also the development and installation of an advanced high voltage (6 MV) laser triggered switch (Fig. 3) [13]. Its inclusion in Z reduced the prefire rates to 0.1%, the jitter to 5 ns, and increased the switch life-time to 90 shots.

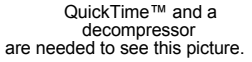

Fig. 3. The new 6-MV switch.

In parallel with the successful Z operation, an impressive number of modeling work has already been done to understand and further enhance its

performance. An advanced 2D circuit model supported by a fully electromagnetic 3D model was successfully constructed and benchmarked with the experimental results, thus providing the first 3D virtual pulsed power accelerator.

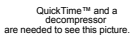

Fig. 4. The pulsed power components sequence of one of the 36 identical power lines feeding the load.

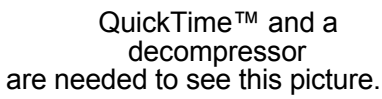

Fig. 5(a) A pictorial representation of the electromagnetic wave propagation through the pulsed power components at a number of time snapshots.

Figure 4 presents the pulsed power sequence of components traveled by the pulse during its propagation from the Marx generator to the vacuum reaction chamber [14]. Figure 5(a) gives a pictorial representation of the electromagnetic wave propagation through the pulsed power components at a number of time snapshots.

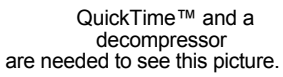

Fig. 5(b). Comparison of the simulation predicted wave forms with the experimentally observed ones at the various locations of the transmission and pulse forming chain.

Fig. 5(b) provides comparison of the simulation predicted wave forms with the experimentally observed ones at the various locations of the transmission and pulse forming chain [15,16]. As mentioned above, there are 18 identical chains like the one presented in Figures 4 and 5. In addition to the creation of the pulsed power virtual accelerator, a number of models were developed to describe the operation of various pulsed power segments of the driver: namely, a new water-dielectric-breakdown model for large area multi-megavolt pulsed-power systems, a statistical model of insulator flashover, a first 3D particle–in-cell (PIC) convolute simulation, a relativistic fluid model of Magnetically Insulated Transmission Line (MITL) electron flow inside the vacuum reaction chamber, a model estimating the energy loss to conductors operating at linear current densities as high as 10 MA/cm, a 2D PIC model of an imploding Z pinch load, and finally a 3D mechanical model of the entire accelerator. The latter is very important for the life duration and mechanical integrity of the machine and necessary to understand and mitigate the distribution of mechanical stresses at the various locations of hardware components during each shot. The energy transmitted to the load during a Z-pinch shot is quite large and approximately equal to that released by the explosion of

~ 0.7 kg TNT.

III. HIGH ENERGY DENSITY PHYSICS RESEARCH ON Z

High energy density science (HEDS) experiments are mounted at the center of Z, as shown in Fig. 6. These experiments usually employ cylindrical wire arrays, liners, magnetized liners, and or short-circuit fixed conductors for isentropic compression experiments (ICE). The current from Z provides a **J x B** force that either implodes a z-pinch load producing radiation or provides magnetic pressure for ICE. The energy conversion efficiency is high for a wire-array implosion, with typical x-ray energy 15% of the stored electrical energy and x-ray power 2 to 4 times the electrical power.

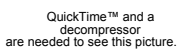

Fig. 6. HEDS experiments are mounted at the center of Z.

Diagnosing the imploding plasma is difficult because of the high-power radiation background, but is possible with x-ray backlighting using a bent-crystal imaging (BCI) detector [17-19] (Fig. 7).

This technique has allowed diagnosis of the details of plasma implosions as well as diagnosis of the spherical symmetry and minute surface details of radiation-driven imploding capsules.

Significant progress has been made in understanding the physics of the z-pinch plasma. The simple model of a thin-shell plasma implosion has been replaced by a more detailed 3D picture with ablated mass from wire arrays, Magnetic Rayleigh-Taylor (MRT) bubbles and spikes, and azimuthal currents of the imploding plasma.

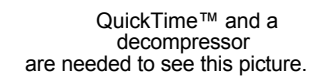

Fig. 7. Two frame monochromatic x-ray backlighter.

Experiment

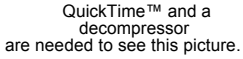

Simulation

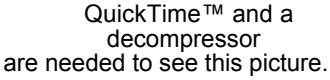

Fig. 8. 3D simulations are in a very good agreement with back-lighter radiographic data of the imploding wire array and the measured x-ray power yield.

These effects have been successfully modeled with the 3D ALEGRA code (Fig. 8).

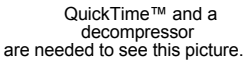

Fig. 9 Pictorial representation of double-ended hohlraum fusion set-up.

Experiments with double-ended hohlraum configurations on Z (Fig. 9) [20] have validated two dimensional (2D) computational models of hohlraum energetics and radiation symmetry for scaling to larger accelerators. Over the last several years, rapid progress has been made evaluating the double-z-pinch indirect-drive ICF high-yield target concept [21]. We have demonstrated efficient coupling of radiation from two wire-array-driven primary hohlraums to a secondary hohlraum that is large enough to drive a high yield ICF capsule. The secondary hohlraum is irradiated from two sides by *z*-pinches to produce high radiation symmetry. This double-pinch source was driven from a single electrical power feed [22] on the *Z* accelerator. The double *z*-pinch has imploded ICF capsules with high radiation symmetry and to high capsule radial convergence ratios of 14–21 [23-25]. Advances in wire-array physics have improved our understanding of *z*-pinch power scaling with increasing drive current. We have also developed and experimentally demonstrated techniques for shaping the *z*-pinch radiation pulse necessary for efficient capsule compression. Figure 10 shows two different radiation pulse shapes achieved with the Z accelerator. The blue trace is the one necessary for efficiently coupling the radiation energy to the capsule. It was obtained by utilizing nested array z-pinches. A nested array configuration includes two wire arrays, where one array is inserted inside another of a larger diameter. In addition to the symmetry and time history of the radiation pulse, the capsule design is also of paramount importance. The materials utilized and the number of layers surrounding the deuterium or tritium to be fused can affect the degree of fuel compression and eventually the thermonuclear ignition (fusion) and yield.

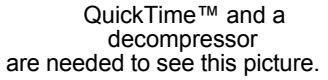

Fig. 10. Two different radiation pulse shapes achieved with the Z accelerator.

Fig. 11 Capsule and secondary hohlraum design for double-ended z-pinch high yield.

520 MJ yield

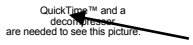

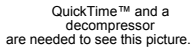

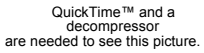

Fig. 12. 2D simulation demonstrating compression of the capsule of Fig. 11.

Figure 11 depicts such a capsule design for ignition and high yield (500 MJ fusion energy released). It shows the wall geometry required to generate the spherically uniform radiation pulse from the reflecting surfaces surrounding the capsule (secondary hohlraum). 2D simulations demonstrate compression and ignition of the capsule (Fig. 12).

In addition to the double *z*-pinch driven fixed

wall hohlraum approach to inertial fusion described above, two more indirect-drive ICF concepts have been explored on the *Z* accelerator [26-67]: the dynamic hohlraum and the single z-pinch static-wall hohlraum.

The dynamic hohlraum (Fig. 13) locates an ICF capsule in a low density foam converter at the center of an imploding *z*-pinch. The wire array implodes onto the foam, creating a source of soft x-rays that couples efficiently to the capsule. Effective capsule drive temperatures of the order of 200 eV can be attained [26, 30, 31, 33]. Experiments with the Z driver have obtained time-resolved x-ray spectra from an imploded ICF core, indicating hot spot temperatures □0.8–1.0 keV [26].

QuickTime™ and a
decompressor
are needed to see this picture.

Fig. 13. Dynamic hohlraum configuration.

The single-pinch static-wall hohlraum harnesses the very high internal brightness temperatures of the dynamic hohlraum drive just prior to stagnation (230 ± 10 eV [37]) to couple 10 TW into a compact hohlraum located directly on the *z*-pinch axis. Hohlraum temperatures of 122 ± 6 eV (155 ± 8 eV) have been developed in 6 mm diameter by 7 mm long (4 mm diameter by 4 mm long) hohlraums [34, 36], the highest temperatures obtained in a stationary secondary driven by a *z*-pinch.

Most recently a new approach to pulsed power driven inertial fusion was proposed by S.A Slutz and coworkers; the Magnetized Liner Inertial Fusion (MagLIF) concept (Fig. 14) [68]. While the previously investigated ICF schemes assume spherically shaped fusion capsule targets, MagLIF relies on cylindrical compression.

QuickTime™ and a
decompressor
are needed to see this picture.

QuickTime™ and a
decompressor
are needed to see this picture.

Fig. 14. The MagLIF process.

The radial convergence required to reach fusion conditions is considerably higher for cylindrical than for spherical implosions since the volume is proportional to r^2 versus r^3, respectively. Fuel magnetization and preheat significantly lowers the required radial convergence enabling cylindrical implosions to become an attractive path toward generating fusion conditions. Numerical simulations indicate that significant fusion yields may be obtained by pulsed-power-driven implosions of cylindrical metal liners onto magnetized (>10 T) and preheated (100–500 eV) deuterium-tritium (DT) fuel. Yields exceeding 100 kJ could be possible on Z at 25 MA, while yields exceeding 50 MJ could be possible with a more advanced pulsed power machine delivering 60 MA. These implosions occur on a much shorter time scale than previously proposed implosions [69], about 100 ns as compared to about 10 μs for Magnetized Target Fusion (MTF). Consequently the optimal initial fuel density (1–5 mg/cc) is considerably higher than for MTF (1 μg/cc). Thus the final fuel density is high enough to axially trap most of the α-particles for cylinders of approximately 1 cm in length with a purely axial magnetic field; i.e., no closed field configuration is required for ignition. According to the simulations, an initial axial magnetic field is partially frozen into the highly conducting preheated fuel and is compressed to more than 100 MG. This final field is strong enough to inhibit both electron thermal conduction and the escape of α-particles in the radial direction. Preheating the fuel reduces the compression needed to obtain ignition temperature and allows relatively low velocity implosions (5-10 cm/μs). Analytical and numerical calculations indicate that the DT can be heated to 200–500 eV with 5–10 kJ of green laser light, which could be provided by the Z-Beamlet laser. The Magneto-Rayleigh-Taylor (MRT)□ instability poses the greatest threat to this approach to fusion. Two-dimensional LASNEX [70] simulations indicate that the liner walls must have a substantial initial thickness □10–20% of the radius□so that they maintain integrity throughout the implosion.

Experimental work has been started to study the MRT instability and benchmark LASNEX code predictions with experimental results [71]. The growth of MRT instability in aluminum liners containing a preseeded axial modulation of the wall thickness and a smooth un-modulated section is being studied with backlighting radiographs.

Fig. 15. Radiographic snapshots of the imploding liner at two times, 55 ns and 77 ns, in the driving current pulse. The growth of the instability is very nicely resolved.

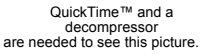

Fig. 16. The radiographic measurements of the MRT instability growth are in excellent agreement with LASNEX simulation results.

The precision and resolution of the images are remarkable (Fig. 15) and in very good agreement with LASNEX predictions (Fig. 16). The radiographs taken at different times during the liner implosion are almost identical to those simulated by LASNEX. This work will help to optimize the liner thickness and materials in order to minimize the disturbing effect of the MRT instability.

Radiation transport in all high temperature mid-atomic number (Z) plasmas is uncertain, by some unknown amount, since opacity measurements are unavailable. Solar interior (Fig. 17) models disagree with observations and this is most probably due to opacity uncertainties. Prior Z opacity measurements reached electron temperatures of $T_e \sim 156$ eV. This enabled testing models for the iron charge states and energy levels found in the sun. However, the densities were still ~ ten times too low. Current opacity measurements have achieved both high densities ($n_e = 2.8 \times 10^{22}$ cm^{-3}) and temperatures ($T_e \sim 190$ eV) [72]. Opacity measurements on Z are now closer to replicating solar interior matter. Although the dynamic hohlraum experiments have achieved the T_e of the sun convective zone (CZ) interior, the densities are smaller by a factor of three (solar convective zone interior density is of the order of $n_e \sim 1 \times 10^{23}$ cm^{-3}).

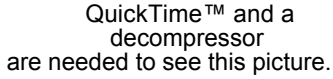

Fig. 17. Solar interior models disagree with observations because of radiation opacity uncertainties.

Independent triggering of the 36 pulse-forming modules of the Z accelerator is used to provide ~ 26 MA, ~ 300-600 ns rise-time shaped current pulses necessary for material dynamics studies at high stresses. The resulting magnetic fields of several megagauss produce quasi-isentropic compression of the short-circuit load conductors over the discharge time of the machine with magnetic pressures exceeding the 6 Mbars [73-75]. Planar stress waves are generated in centimeter-sized material samples.

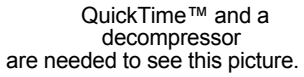

Fig. 18. The ICE load geometry.

Typically, four anode panels are arranged about a central stainless steel or tungsten rectangular cathode post (Fig.18), forming a symmetric anode-cathode (A-K) gap with exactly parallel surfaces.
3D magneto hydrodynamic (MHD) calculations show that magnetic field uniformity of 0.5% can be obtained over the central horizontal region of each anode plate of the cubic geometry of the load [76]. Up to five samples can be stacked vertically on a panel. The magnetic pressure induces a hydrodynamic stress

wave that propagates into the anode material that can be used in isentropic compression experiments (ICE). An example of the ICE technique is found in references [77, 78], where the high-pressure compression response of aluminum is inferred by measuring its stress up to 2.5 Mbars. Since ramp loading produces continuous loading curves, the measured stress–strain response is sensitive to small changes in material response. Thus the technique is well suited for the study of first-order phase transitions.

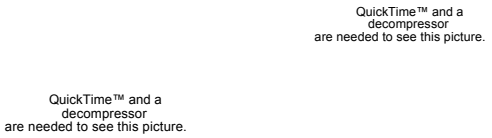

Fig. 19. ICE (left) and flyer plate (right) samples.

A successful spin-off of the ICE technique has been developed to magnetically accelerate flyer plates to ultrahigh velocities [79]. The technique uses the magnetic field produced in the A-K gap to impulsively load the anode, providing momentum and launching it as an effective flyer plate to high velocity (Fig.19).
The highest velocity achieved to date is 45 km/s. This is an accepted technology to study the various material response under extreme shock forces (Hugoniot). The flyer plate strikes the sample and launches a shock wave that propagates under non-isentropic conditions, which means that the pressure wave causes an increase in the temperature and density inside the material.

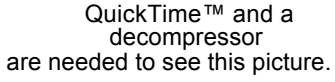

Fig. 20 The Hugoniot and Isentropic compression paths.

Figure 20 pictorially explains the difference between isentropic and Hugoniot compression. Figure 21 presents the different effect of the two modes of compressions on a material.

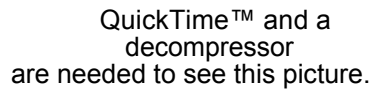

Fig.21. Behavior of a material under Hugoniot and Isentropic compression conditions.

The magnetically accelerated flyer plate technique has been used to help resolve a controversy in the compressibility of hydrogen and its isotopes at high pressure. Flyer plate experiments have also been performed to obtain Hugoniot data for beryllium and diamond.

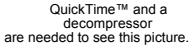

Fig. 22. Stress versus density for diamond. The accuracy of measurements is better than 1%.

Figure 22 demonstrates the high precision capability of these experiments on Z. The results are in excellent agreement with numerical QMD simulations [79]. A significant benefit of the ultra-high velocity flyer plate technique is the ability to perform complex loading experiments at extreme pressures. Experiments can be performed with composite flyer plates, fabricated with layers of material with different shock impedance, capable of imparting finite duration shock loading followed by well defined pressure release. By measuring the shock and release wave profiles through multiple thicknesses of the sample, the wave speed of the material in the shocked state can be inferred by a wave overtake method [80]. The wave speed is sensitive to the state of the material, with a solid exhibiting a noticeably higher wave speed than a liquid. By measuring the wave speed over a span of Hugoniot pressures, the shock pressure at which melt begins can be determined.

IV. SELECTED APPLICATIONS OF PULSED POWER TECHNOLOGY

During the last few years Sandia has significantly advanced the state of the art of high energy and high brightness radiographic sources. The main test bed for this research is the Radiographic Integrated Test Stand (RITS-6) [81].

RITS-6 (Fig. 23) is an Inductive Voltage Adder (IVA) accelerator developed specifically for driving high brightness flash x-ray radiographic sources. The x-ray sources are high-power electron beam diodes. In its present configuration, six induction cavities are driven by two, 8-ohm, parallel water-dielectric pulse forming lines (PFLs). The individual induction cavities are joined in series by a vacuum coaxial magnetically insulated transmission line (MITL) that delivers power from the cavities to the diode region. The geometry of the accelerator and diode region is shown in Fig. 23. RITS-6 is capable of producing 7-11 MeV, 125-190 kA, 75-ns-pulse-length electron beams. These beams are focused onto high-Z x-ray converter targets with power densities in excess of 10 TW/cm^2.

Advanced time-resolved diagnostics have been developed and implemented to measure the x-ray spot size, the radiographic resolution, and the x-ray dose as a function of time. Doses of 350 rad at 1m from the source have been measured generated from a 55 ns duration radiation pulses emanating from 2.6 mm spot size x-ray sources (Fig. 24).

QuickTime™ and a decompressor are needed to see this picture.

Fig. 24. Radiographic x-ray spot size.

The sources are optimized with the aid of 3D code simulations like the one shown in Figure 25 for the parapotential electron diode. In this diode, the electron beam is focused by a low-pressure gas cell placed before the converter x-ray target.

QuickTime™ and a decompressor are needed to see this picture.

Fig. 23. The Radiographic Integrated Test Stand (RITS-6).

QuickTime™ and a decompressor are needed to see this picture.

Fig. 25. 3D simulations of a parapotential x-ray electron diode.

Although the Z-pinch research is focused on single-shot ICF and HED studies, a future dream is the utilization of inertial confinement fusion for energy

production. The long-range goal of z-pinch IFE is to produce an economically attractive power plant using high-yield z-pinch-driven targets (3 GJ) in a relatively low rep-rate (0.1 Hz) system. The present concept for a Z-IFE power plant uses a repetitive pulsed power driver (linear transformer driver, LTD), a recyclable transmission line (RTL), a dynamic hohlraum z-pinch-driven target, and a thick liquid-wall chamber. The RTL connects the pulsed power driver directly to the z-pinch-driven target, and is made from frozen flibe or a material that can be easily separated from the flibe (such as low activation ferritic steel). The fusion explosion destroys the RTL, but the RTL materials are recycled, and a new RTL is inserted on each shot together with the fusion target. An artist's conceptual representationof the elements of a 1000 MWe power plant is shown in Fig. 26.

The IFE research effort, although modestly funded through the last few years, has nonetheless achieved substantial understanding and advances in most of the key elements of Z-IFE. The research has been focused on (1) RTLs, (2) repetitive pulsed power drivers, (3) shock mitigation (because of the high-yield targets), (4) planning for a proof-of-principle full RTL cycle demonstration with a 2 MA, 1 MV, 100 ns, 0.1 Hz driver, (5) IFE target studies for multi-GJ yield targets, and (6) z-pinch IFE power plant engineering and technology development. A considerable portion of the research has been concentrated on two critical components of this concept, the RTLs and the repetitive pulsed power driver [82].

Key physics issues for RTLs involving the power flow at the high linear current densities that occur near the target (up to 5 MA/cm) have been investigated. These issues include surface heating, melting, ablation, plasma formation, electron flow, magnetic insulation, conductivity changes, magnetic field diffusion changes, possible ion flow, and RTL mass motion. These issues

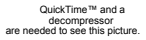

Fig. 26. Conceptual elements of a 1000 MWe power plant

have been studied theoretically, computationally, and experimentally. Present results indicate that RTLs could work at 5 MA/cm or higher, with anode-cathode gaps as small as 2 mm. An RTL misalignment sensitivity study has been performed using a 3D circuit model. The load current variations are small for significant RTL misalignments. The structural issues for RTLs have also been addressed.

Sandia has a program focused on the development of high current, high voltage, fast (100 ns) rep-rated drivers based on the Linear Transformer Driver (LTD) technology [83-90]. This technology could revolutionize the architecture of the pulse power devices of the future. The LTD approach can provide very compact devices that can deliver very fast high current and high voltage pulses straight out of the cavity without any complicated pulse forming and pulse compression network. Through multistage inductively insulated voltage adders, the output pulse, increased in voltage amplitude, can be applied directly to the load. Because the output pulse rise time and width can be easily tailored to the specific application needs, the load may be a vacuum electron diode, a z-pinch wire array, a gas puff, a liner, an ICE load or an IFE target.

The LTD technology is very robust and simple. The main components are a switch, a capacitor and a ferromagnetic core. The extreme modularity of the technology provides immunity to faults and assures graceful degradation. The pulse forming capacitors and switches are enclosed inside an accelerating cavity. An LTD cavity can produce large current outputs by feeding each inductive cavity core with many capacitors connected in parallel in circular arrays. In principle currents of up to 2 MA can be obtained. The limitation is the size of the cavities. With the present capacitor and switch dimensions, it cannot in practice exceed 3-4 meters in diameter, since a cavity then becomes cumbersome and difficult to handle. If larger currents and higher voltages are required, voltage adder modules of many LTD cavities can be connected in parallel to the load. Utilizing the presently available capacitors and switches, we can envision building the next generation of fast pulsed power drivers without large Marx generators and voluminous oil-water tanks and pulse forming and pulse compression networks as is the case with the present technology drivers. The LTD devices can be multi-pulsed with a repetition rate up to 0.1 Hz or higher as required for the IFE driver power plants. Two prototype 0.5 MV LTD cavities have been built and successfully operated in single and in rep-rated modes. The demonstrated energy efficiency (75% wall plug to load), the very small jitter (< 2 ns), and the reproducibility of the output pulse (Fig. 27) of those devices are beyond match by any other device.

QuickTime™ and a
decompressor
are needed to see this picture.

Fig. 27 Overlay of 200 consecutive shots.

QuickTime™ and a
decompressor
are needed to see this picture.

Fig. 28 1-MA, 100-GW, 70 ns LTD cavity (top flange removed).

Figure 28 shows the interior of one 1 MA cavity while Fig. 29 shows the output pulse. It contains 40 switches and 80 capacitors arranged in two circular arrays (one on the top of the other). The cavities were tested individually and in 5-cavity vacuum insulated voltage adders. The loads utilized were resistors and electron vacuum diodes (Fig. 30) [90].

Fig. 29. Current, voltage and power output pulses of the

Fig. 30. 5, 1-MA LTD cavity voltage adder with the cylindrical cathode stock and visible outside of the cavities

QuickTime™ and a
decompressor
are needed to see this picture.

The combination of multiple LTD voltage adder coaxial lines into a tri-plate and then into bi-plate RTL transmission line has been examined [83,84]. 3D codes were used to study the electron flow losses near the magnetic nulls that occur where coax transmission lines are added together. LTD architectures for Z-IFE high yield facilities have also been developed. Results from power flow studies validated the LTD/RTL concept for single-shot ICF high yield and for repetitive-shot IFE.

QuickTime™ and a
decompressor
are needed to see this picture.

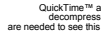

Fig. 31. Sixty-cavity water insulated LTD voltage adder

Very high current LTD drivers will contain many voltage adders connected in parallel. In order to obtain the required high voltage, each voltage adder will be composed of a large number of LTD cavities. Fig. 31 shows a 60-cavity voltage adder module which is the building block for our pettawatt-class LTD z-pinch driver (Fig. 32) [91]. It contains 210 modules and also includes a center section water transformer to increase the output voltage from the 6 MV at the end of the modules to the 20 MV required by the load.
Another great attribute of the LTD accelerators is their ability to tailor the output pulse shape according to the requirements of the different applications. Numerical studies have demonstrated the flexibility of the fast LTDs to produce output pulses of varied rise times and FWHM [92]. This can be accomplished by staggering the triggering of the cavities according to a predetermined schedule. An even finer tuning of the output pulse can be achieved by varying the firing of each cavity quadrant.

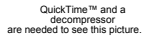

Fig. 32. LTD Petawatt driver

Fig. 33. The new Mykonos LTD Laboratory

Experiments with a 1 TW module, which will include 10, 1-MA LTD cavities connected in series, are in preparation at the MYKONOS LTD laboratory at Sandia National Laboratories. The MYKONOS voltage adder will be the first ever IVA built with a transmission line insulated with de-ionized water. Presently we have assembled and are testing a two-cavity water insulated voltage adder (Fig. 33). This is the first step towards the completion of the 10-cavity, 1-TW module. In addition, one of the 0.5-MA LTD cavities is currently serving as a test bed for evaluating a number of different types of switches, resistors, alternative capacitor configurations, cores and other cavity components.

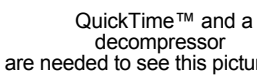

Fig. 34. The 1-MV, 150-kA radiographic LTD accelerator

The compactness, the single stage pulse compression, the closed geometry, and the minimum infrastructure needs make the LTD technology very attractive for smaller current radiographic accelerators. They are an ideal fit to operate at remote areas where infrastructures are minimal or non-existent. A proof of principle 1-MV, 150 kA radiographic LTD accelerator composed of 7 smaller, 20 capacitor cavities (Fig. 34) has been built and operated with a vacuum electron diode as a load. The successful performance of this device motivated the construction of 14 more of these cavities in order to upgrade the assembly to 3 MV (Fig. 35).

.

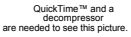

Fig. 35. Design of the 3-MV radiographic LTD accelerator.

A spin off of the LTD technology is the development of a new pulsed-power driver uniquely fit to produce on demand the most elaborate pulse shapes. This unique capability is achieved by utilizing genetic algorithms to program the firing sequence of the switches. Figure 36 shows an artist's conception of this

device, named GENESIS [93]. It looks like a giant LTD cavity containing 480 capacitors (240 bricks) delivering a 5-MA current to an ICE load. Its operation would be completely dedicated to isentropic compression experiments.

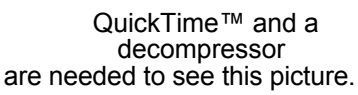

Fig. 36. Conceptual design of the GENESIS ICE driver

Figure 37 presents examples of some of the potential output wave-forms achievable with GENESIS and the switch triggering times.

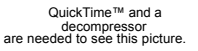

Fig. 37. Examples of GENESIS output pulses and the corresponding triggering times.

V. SUMMARY

A combination of theory, simulations, and high quality experiments has enabled significant progress in high energy density science and related applications. This progress has been enabled by the development of new pulsed-power platforms and the related theory and computations that have supported and guided experiments. The Z accelerator has been a very successful experimental platform for performing HED science. It made important contributions to ICF research, benefiting the national efforts in this endeavor. Dynamic material property studies have reached a new level of precision and capability on Z. Research in radiation hydrodynamics and radiation effects has benefited from the x-ray radiation produced by the high temperature plasmas generated in the load regions of Z. Compact machines are being developed to enable inexpensive and more precise dynamic materials research. A program to grow the fundamental science studies on Z is under way. The combined refurbished Z, Z-Beamlet, and Z-Petawatt provides an exciting experimental platform for high quality fundamental science research. The LTD technology is very promising, and it is being pursued for many pulsed power applications, especially for radiography and for the next generation of high current drivers for HED and IFE applications. We have developed conceptual designs of new driver architectures that take advantage of the high reliability, simplicity, compactness, and new capabilities enabled by the LTD pulsed power technology.

ACKNOWLEDGEMENT

Sandia is a multi-program laboratory operated by Sandia Corporation, a Lockheed Martin Company, for the United States Department of Energy's National Nuclear Security Administration under Contract DEAC04-94AL85000.

REFERENCES

[1] R. B. Spielman *et al.*, in *Proceedings of the 11th IEEE International Pulsed Power Conference*, edited by G. Cooperstein and I. Vitkovitsky (IEEE, Piscataway, NJ, 1997), p. 709.
[2] P. Corcoran, *et al.*, *ibid.*, p. 466.
[3] R. J. Garcia, *et al.*, *ibid*., p. 1614.
[4] H. C. Ives, *et al.*, *ibid.*, p. 1602.
[5] R. W. Shoup, *et al.*, *ibid*., p. 1608.
[6] D. L. Smith, *et al.*, *ibid.*, p. 168.
[7] K. W. Struve, *et al.*, *ibid.*, p. 162.
[8] W. A. Stygar, *et al.*, *ibid.*, p. 591.
[9] W. A. Stygar, *et al.*, *ibid.*, p. 1258.
[10] E. A. Weinbrecht *et al.*, in *Proceedings of the 16th*

IEEE International Pulsed Power Conference, edited by E. Schamiloglu and F. Peterkin (IEEE, Piscataway, NJ, 2007), p. 975.
[11] M. E. Savage *et al.*, *ibid.*, p. 979.
[12] K. W. Struve *et al.*, *ibid.*, p. 985.

[13] K. LeChien *et al.,* Phys. Rev. ST Accel. Beams **11,** 060402 (2008).
[14] D. V. Rose, *et al.*, Phys. Rev. ST Accel. Beams **13**, 010402 (2010).
[15] D. Rose, D. Welch *et al.*, in Proceedings of the 7th International Conference on Dense Z-Pinches, edited by D, A. Hammer and B. R. Kusse (AIP, Melville, NY 2009), p. 263.
[16] D. Rose, D. Welch *et al.*, Phys. Rev. ST Accel. Beams **13**, 040401 (2010).
[17] D. B. Sinars, G.R. Bennett, D.F. Wenger, M.E. Cuneo, and J.L. Porter, Appl. Optics **42**, 4059 (2003).
[18] D. B. Sinars, G.R. Bennett, D.F. Wenger, *et al.*, Rev. Sci. Instrum. **75**, 3672-3677 (2004).
[19] G. R. Bennett, D.B. Sinars, D. F. Wenger, *et al.*, Rev. Sci. Instrum. **77**, 10E322 (2006).
[20] M. E. Cuneo, R. A. Vesey, G. R. Bennett, *et al.*, Plasma Phys. Control. Fusion **48**, R1 (2006).
[21] J. H. Hammer *et al., Phys. Plasmas* **6**, 2129 (1999).
[22] M. E. Cuneo *et al., Phys. Rev. Lett.* **88**, 215004 (2002).
[23] G. R. Bennett *et al., Phys. Rev. Lett.* **89**, 245002 (2002).
[24] G. R. Bennett *et al., Phys. Plasmas* **10**, 3717 (2003).
[25] R. A. Vesey *et al., Phys. Plasmas* **10**, 1854 (2003).
[26] J. E. Bailey *et al., Phys. Rev. Lett.* **92**, 085002 (2004).
[27] C. L. Ruiz *et al., Phys. Rev. Lett.* **93**, 015001 (2004).
[28] V. P. Smirnov *et al., Plasma Phys. Control. Fusion* **33**, 1697 (1991).
[29] J. H. Brownell *et al., Phys. Plasmas* **5**, 2071 (1998).
[30] T. J. Nash *et al., Phys. Plasmas* **6**, 2023 (1999)
[31] S. A. Slutz *et al., Phys. Plasmas* **8**, 1673 (2001).
[32] J. E. Bailey *et al., Phys. Rev. Lett.* **89**, 095004 (2002).
[33] S. A. Slutz *et al., Phys. Plasmas* **10**, 1875 (2003).
[34] T. A. Mehlhorn *et al., Plasma Phys. Control. Fusion* **45** A325, (2003).
[35] T. W. L. Sanford *et al., Phys. Rev. Lett.* **83**, 5511 (1999).
[36] R. E. Olson *et al., Fusion Technol.* **35**, 260 (1999).
[37] T. W. L. Sanford *et al., Phys. Plasmas* **7**, 4669 (2000).
[38] T. W. L. Sanford *et al., Plasma Phys. Control. Fusion* **46** B42, (2004).
[39] J. L. Porter Jr., *Bull. Am. Phys. Soc.* **42**,1948 (1997).
[40] K. L. Baker *et al., Appl. Phys. Lett.* **75**, 775 (1999).
[41] R. E. Chrien *et al., Rev. Sci. Instrum.* **70**, 557 (1999).
[42] R. E. Chrien *et al., Bull. Am. Phys. Soc.* **44**, 52 (1999).
[43] M. E. Cuneo *et al., Bull. Am. Phys. Soc.* **44**, 40 (1999).
[44] R. A. Vesey *et al., Bull. Am. Phys. Soc.* **43**, 1903 (1998).
[45] R. A. Vesey *et al., Bull. Am. Phys. Soc.* **49**, 227 (1999)
[46] R. A. Vesey *et al., Bull. Am. Phys. Soc.* **45**, 360 (2000).
[47] K. L. Baker *et al., Phys. Plasmas* **7**, 681 (2000).
[48] M. E. Cuneo *et al., Phys. Plasmas* **8**, 2257 (2001)
[49] M. E. Cuneo *et al., Laser Part. Beams* **18**, 481 (2001).
[50] D. L. Hanson *et al., Phys. Plasmas* **9**, 2173 (2002)
[51] R. A. Vesey *et al., Inertial Fusion Sciences and Applications 2001* edited by K. A. Tanaka *et al* (Paris: Elsevier) p. 681 (2002).
[52] R. A. Vesey *et al., Phys. Rev. Lett.* **90**, 035005 (2003).
[53] R. A. Vesey *et al., Phys. Plasmas* **10**, 1854 (2003).
[54] G. R. Bennett *et al., Phys. Plasmas* **10**, 3717 (2003).
[55] D. A. Callahan *et al., Nucl. Instrum. Methods* A **544** 9, (2005).
[56] D. A. Callahan *et al., Plasma Phys. Control. Fusion* **47** B379, (2005).
[57] M. E. Cuneo *et al., Bull. Am. Phys. Soc.* **46**, 234 (2001).
[58] M. E. Cuneo *et al., 5th Conf. on Dense Z-Pinches (Albuquerque, NM, 23–28 June 2002)* (unpublished) (2002).
[59] M. E. Cuneo *et al., Phys. Rev.* E **71,** 046406 (2005).
[60] W. A. Stygar *et al., Phys. Rev.* E **69**, 046403 (2004).
[61] E. M. Waisman *et al., Phys. Plasmas* **11**, 2009 (2004).
[62] D. B. Sinars *et al., Rev. Sci. Instrum.* **75**, 3673 (2004).
[63] D. B. Sinars *et al., Phys. Rev. Lett.* **93**, 145002 (2004).
[64] D. B. Sinars *et al., Phys. Plasmas* **12**, 056503 (2005).
[65] M. E. Cuneo *et al., Phys. Rev. Lett.* **94**, 225003 (2005).
[66] W. A. Stygar *et al., Phys. Rev.* E **72**, 026404 (2005).
[67] M. E. Cuneo *et al., Phys. Rev. Lett.* **95**, 185001 (2005).
[68] S. A. Slutz *et al.,* 2003 *Phys. Plasmas* **17**, 056303 (2010).

[69] I. R. Lindemuth and R. C. Kirkpatrick, Nucl. Fusion **23**, 263 (1983)
[70] G. B. Zimmerman and W. L. Kruer, Comm. Plas. Phys. Contr. Fusion **2**, 51 (1975).
[71] D. B. Sinars *et al., Phys. Rev. Lett.* **105**, 185001 (2010).
[72] J. E. Bailey *et al., Phys. Rev. Lett.* **99** 265002 (2007).
[73] J. R. Asay, in *Shock Compression of Condensed Matter – 1999*, edited by M.D. Furnish, L. C. Chhabildas, and R. S. Hixson (AIP, New York, 1999) p. 261.
[74] R. W. Lemke, M. D. Knudson, A. C. Robinson, T. A. Haill, K. W. Struve, J. R. Asay, and T. A. Mehlhorn, Phys. Plasmas **10**, 1867 (2003).
[75] D. B. Reisman, A. Toor, R. C. Cauble, C. A. Hall, J. R. Asay, M. D. Knudson, and M. D. Furnish, J. Appl. Phys. **89**, 1625 (2001).
[76] J. P Davis, J. Appl. Phys. **99**, 103512 (2006).
[77] D. B. Hayes and C. A. Hall, in *Shock Compression of Condensed Matter – 2001*, edited by M.D. Furnish, N. Thadhani, and Y. Horie (AIP, New York, 2001) p. 1177.
[78] D. A. Dolan, M. D. Knudson, C. A. Hall, and C. Deeney, Nature Physics **3**, 339 (2007).
[79]M. D. Knudson, M. P. Dejarlais, D. H. Dolan, Science **322**, (2008)**.**
[80] R. G. McQueen, J. W. Hopson, and J. N. Fritz, Rev. Sci. Instrum. **53**, 245 (1982).
[81] I. D. Smith, *et al.*, Proc. 12th IEEE Intl. Pulsed Power Conf., Monterey, CA 1999, p. 403.
[82] C. L. Olson, *et al.,* "Recyclable Transmission Line (RTL) and Linear Transformer Driver (LTD) Development for Z-Pinch Inertial Fusion Energy (ZIFE) and High Yield," Sandia National Laboratories Report, SAND2007-0059, January 2007.
[83] M. G. Mazarakis *et al.,* Phys. Rev, ST Accel. Beams **12**, 050401 (2009).
[84] M. G. Mazarakis and C. L. Olson, in Proceedings of the 21st IEEE/NPSS Symposiumon Fusion Engineering (SOFE 2005), edited by Oak Ridge National Laboratory (IEEE, Piscataway, NJ, 2005), paper 02–09, # 05CH37764C.
[85] M. G. Mazarakis and R. B. Spielman, in Proceedings of the 12th IEEE International Pulsed Power Conference, edited by C. Stallings and H. Kirbie (IEEE, Piscataway, NJ, 1999), p. 412, # 99CH36358.
[86] A. A. Kim, A. N. Bastrikov, S.N. Volkov, V.G. Durakov, B. M. Kovalchuk, and V. A. Sinebryukhov, in Proceedings of the 13th International Symposium on High Current Electronics, edited by Boris Kovalchuk and Gennady Remnev (IHCE SB RAS, Tomsk, Russia, 2004), p. 141.
[87] M. G. Mazarakis, W. E. Fowler, F.W. Long, D. H. McDaniel, C. L. Olson, S. T. Rogowski, R. A. Sharpe, and K.W. Struve, in Proceedings of the 15th IEEE International Pulsed Power Conference, edited by J. E. Maenchen and E. Schamiloglu (IEEE, Piscataway, NJ, 2005), p. 390, # 05CH37688C.
[88] M. G. Mazarakis, R. B. Spielman, K.W. Struve, and F.W. Long, ''A New Linear Inductive Voltage Adder Driver for the Saturn Accelerator,'' 20th International Linear Accelerator Conference, Monterey, California, August 2000. Also presented in the 1st International Conference on Radiation Physics, High Current Electronics, and Modification of Materials, Tomsk, Russia, 2000.
[89] M. G. Mazarakis, R. B. Spielman, K.W. Struve, and F.W. Long, in Proceedings of the 13th IEEE International Pulsed Power Conference, edited by R. Reinovsky and M. Newton (IEEE, # 01CH37251, Piscataway, NJ, 2001), p. 587.
[90] A. A. Kim, M.G. Mazarakis, V.A. Sinebryukhov, B.M. Kovalchuk, V.A. Visir, S.N. Volkov, F. Bayol, A.N. Bastrikov, V.G. Durakov, S.V. Frolov, V.M. Alexeenko, D. H. McDaniel, W. E. Fowler, K. LeChien, C. Olson, W.A. Stygar, K. W. Struve, J. Porter, and R.M. Gilgenbach, Phys. Rev. ST Accel. Beams **12,** 050402 (2009).
[91] W. A. Stygar, M. E. Cuneo, D. I. Headley, H. C. Ives, R. J. Leeper, M.G. Mazarakis, C. L. Olson, J. L. Porter, T. C. Wagoner, and J. R. Woodworth, Phys. Rev. ST Accel. Beams 10, 030401 (2007).
[92] W. A. Stygar, E. E. Fowler, K. R. LeChien, F. W. Long, M.G. Mazarakis, G. R. McKee, J. L. McKenney, J. L. Porter, M. J. Savage, B. S. Stoltzfus, D. M. Van De Valde, and J. R. Woodworth, Phys. Rev. ST Accel. Beams **12**, 030402 (2009).
[93] S.F. Glover, L.X. Schneider, K.W. Reed, G.E. Pena, J.-P. Davis, C.A. Hall, R.J. Hickman, K.C. Hodge, J.M. Lehr, D.J. Lucero, D.H. McDaniel, J. G. Puissant, J.M. Rudys, M.E. Sceiford, S.J. Tullar, D.M. Van De Valde, and F.E. White, "Genesis: A 5 MA programmable pulsed power driver for isentropic compression experiments." *IEEE Transactions on Plasma Science*, 38,No 1, p. 2620 (2010).